Supporting Information

Martin et al. 10.1073/pnas.1321719111

SI Materials and Methods

Field Sampling. Field samples were collected during two cruises, OC443 along 65°W (April 2008) and BLATZ-II from Woods Hole to Bermuda (April 2012). Seawater for bulk particle chemical measurements was collected with Niskin bottles on a conductivity-temperature-depth (CTD) rosette equipped with a fluorometer: 1–4 L were filtered for lipid analysis (OC443, 0.2-μm PVDF filters; BLATZ-II, ∼0.7-μm glass fiber GF/F filters and 0.2-μm PVDF filters), and total particulate P (TPP) and polyphosphate (polyP) (on BLATZ-II only, GF/F). Filters were flash-frozen in LN_2 and stored frozen (lipid samples at −80 °C) until analysis. Two to sixteen liters were filtered onto 0.2-μm polycarbonate filters for cell sorting (BLATZ-II only), fixed in 1% formaldehyde for 20 min, flash-frozen, and stored at −80 °C. Soluble reactive P (SRP) samples were filtered (0.2 μm Sterivex) in the temperate western North Atlantic (TWNA) but not the Sargasso Sea, stored at −20 °C, and analyzed using standard methods; south of the Gulf Stream, additional samples for quantification after MAGIC preconcentration (1) were taken. Wide-aperture, surface-tethered net sediment traps (2) were deployed on BLATZ-II to collect sinking particles; they are designed to collect representative samples of the flux rather than quantify it exactly, but we note that our TPP fluxes are consistent with reports from a nearby time-series site (3). Three traps were deployed successively for 24 h each in both the TWNA and the Sargasso Sea. Trap samples were screened through 363-μm Nitex to remove live zooplankton, split in a rotary splitter, and filtered onto GF/F filters.

Flow-Cytometry Cell Sorting. Samples were thawed at room temperature, gently inverted to resuspend cells off the filter, and prescreened through a 40-μm mesh. They were then sorted on a Becton Dickinson (formerly Cytopeia) Influx Mariner cell sorter. Samples were excited with a 200-mW 488-nm Coherent Sapphire laser. Cellular chlorophyll (692/40 band pass) and phycoerythrin (572/27 band pass) fluorescence were quantified and used in conjunction with forward light scatter to identify *Synechococcus* populations using standard methods (4–6). Sorted aliquots were stored at 4 °C until the entire sample was sorted, and then combined and syringe-filtered onto 0.2-μm polycarbonate (polyP) or 0.2-μm PVDF (lipids) filters, flash-frozen, and stored at −80 °C until analysis. Before filtering, a small aliquot of the sorted cells was removed to confirm cell enumeration in sorted samples; cell abundances were used to calculate polyP per cell. Procedural blanks for polyP and lipid analysis were prepared by filtering sheath fluid collected at the outflow of the flow cytometer through the appropriate filter type, but our target analytes were not detected. To calculate polyP:TPP, the *Synechococcus* cellular P quotas were estimated based on reports from the subtropical western North Atlantic (7); for polyP measurements in the Sargasso Sea, we used the average cellular P quotas from inside an anticyclonic and a cyclonic eddy whereas, for TWNA data, we used the twofold higher cellular P quota reported from inside a mode-water eddy.

Chemical Analyses. Lipids were extracted and quantified by liquid chromatography triple quadrupole mass spectrometry as described (8). On BLATZ-II, lipid samples were taken on PVDF and GF/F filters north of 38°N and at 33°N; samples in between were taken only on PVDF filters. However, where samples were taken on both filters, the sulfoquinovosyldiacylglycerol (SQDG): phosphatidylglycerol (PG) ratio was linearly related (Fig. S6). We used this relationship to calculate a GF/F equivalent value for all SQDG:PG measurements from PVDF samples taken on BLATZ-II; Fig. 1 shows these GF/F equivalent data. The offset in SQDG:PG between filter types was much smaller than the latitudinal variation and was probably caused by GF/F filters not capturing (PG-rich) heterotrophic bacteria quantitatively (9).

TPP was analyzed by $K_2S_2O_8$ wet oxidation followed by standard colorimetric measurement (10). Complete oxidation efficiency was confirmed using glucose-6-phosphate.

Particulate organic carbon (POC) was measured on a Finnigan-MAT DeltaPlus stable light isotope ratio mass spectrometer at Woods Hole Oceanographic Institution using acetanilide as an external standard.

Alkaline phosphatase activity was measured on particles collected onto 0.2-μm filters (2008 cruise), or in unfiltered seawater samples (2012 cruise). Samples were incubated in 96-well plates with saturating concentrations of either the substrate 6,8-difluoro-4-methylumbelliferyl phosphate (2008 cruise) or 4-methylumbelliferyl phosphate (2012 cruise). Fluorescence was measured on a microwell plate reader over the linear range of the assay against a standard curve to calculate maximal rates of uptake (11).

PolyP was determined fluorometrically with 2,6-diamidino-2-phenylindole, after boiling and enzymatic digestion (DNase+RNase, proteinase K) of a subsample from each filter, and expressed as equivalents of the molar amount of P in a synthetic polyP standard (12). Fluorescence was measured at 550 nm upon excitation at 415 nm. Matrix effects were accounted for by standard addition to each sample. We consider this method to give a relative, not absolute, measure of polyP concentration because the synthetic standard (total P content confirmed by hydrolysis and P determination) appears to fluoresce less brightly than natural polyP in our environmental plankton samples. Thus, samples from the Sargasso Sea invariably contained more equivalents of the standard than the molar concentration of TPP, yielding ratios greater than 1. Analysis of fresh subsamples using snake venom phosphodiesterase (Sigma Aldrich) in place of DNase+RNase yielded a 1:1 relationship to the data presented here (Fig. S4), suggesting that residual nucleic acid–polyP complexes are unlikely to be responsible (13). Analysis of a third set of subsamples using 0.25 M NaOH extraction (14) yielded lower values, but the same latitudinal trend reported above (Fig. S5). However, we found this method unsuitable for high-sensitivity analysis of small sample quantities because the strong base must be neutralized exactly with HCl and then heavily diluted with neutral buffer to ensure a suitable pH and salt concentration for staining. Fluorescence signals in NaOH extracts were therefore lower, especially between 38°N and 34°N, where only very small subsamples could be analyzed. More importantly, standard addition indicated more substantial and erratic matrix effects in the NaOH-extracted samples than with enzyme digestion, probably because of insufficient dilution and/or pH adjustment. NaOH extraction was therefore out of the question for flow-sorted samples. It is probably more suitable for analysis of larger sample quantities that allow for greater dilution, such as the sediments for which the NaOH method was developed (14). However, it is unlikely that alkali extraction alone quantitatively extracts all polyP (15), which might partly account for the lower values we obtained using this method. Overall, it seems likely that our enzymatic method at present fails to break down some form of complex between polyP and another macromolecule that has enhanced fluorescence in the presence of DAPI compared with just polyP. The high fluorescence is certainly not due to a matrix effect; matrix effects were accounted for in every sample by

standard addition, and in fact were responsible for a 10–20% reduction in fluorescence compared to the pure standard. Neither is the high fluorescence likely to be due to fluorescence from DAPI interacting with other constituents of biomass, because deep chlorophyll maxima (DCM) samples, containing as much biomass as surface samples, contained very little polyP. Likewise, biomass-rich coastal samples contained low levels of polyP. Moreover, we can rule out any background fluorescence, as background fluorescence was measured in each sample in the absence of DAPI and subtracted.

***Synechococcus* Cultures.** Axenic *Synechococcus* WH8102 was obtained from John Waterbury (Woods Hole Oceanographic Institution) and grown in glass Erlenmeyer flasks in SN medium with 45 μM KH_2PO_4 at 30 μmol photons·m^{-2}·s^{-1} and 23 °C. The SN medium base was 0.2 μm filtered surface seawater from the Sargasso Sea mixed in a 3:1 ratio with deionized (MilliQ) water. Replicate cultures (three each for –P and Refeed, two for +P) were established from a log-phase inoculum. +P cultures started with 45 μmol·L^{-1} P, -P, and Refeed cultures with 1 μmol·L^{-1}. Fluorescence was assessed daily starting on day 11. Samples for flow cytometry (in 1% formaldehyde) and for polyP, TPP, and lipid analysis (filtered onto GF/F filters) were taken daily once growth (as judged by fluorescence) in P-limited cultures had ceased. Samples were flash-frozen and stored at −80 °C. $K_2H_2PO_4$ was added to Refeed cultures to a final concentration of 45 μmol·L^{-1} 24 h before the last set of samples were taken. Procedural blanks for chemical measurements were prepared by filtering blank 45 μmol·L^{-1} P medium through GF/F filters. These procedural blanks contained no lipids or polyP but did contain P carried over from the medium. These P blanks were subtracted from +P and Refeed cultures, but we subtracted only the lower reagent P blank from –P cultures because carryover of dissolved P in P-limited cultures would have been very low. TPP might thus have been overestimated in –P cultures, which would have led us to underestimate their polyP:TPP ratio. Because the –P cultures had the highest polyP:TPP, this underestimate does not impact our conclusions. Cells were enumerated on a Millipore Guava EasyCyte flow cytometer, and chemical measurements were performed as described above. Cellular lipid, polyP, and TPP quotas were stable over the final four sampling days, so measurements taken during this period were averaged for each individual replicate. These averages were then used to calculate the overall treatment mean ± SD, which is thus based on $n = 3$ (−P cultures) or $n = 2$ (+P cultures). For Refeed cultures, only the measurements taken on the final day of sampling (i.e., 24 h after P addition) are reported; data from the Refeed cultures before P addition were indistinguishable from –P cultures.

Estimating Lipid Contribution to C:P Gradient. In the TWNA, mixed-layer TPP averaged 130 ± 17 nmol·L^{-1}, with P-lipids contributing 15 ± 1.1 nmol·L^{-1}, or 11%. In the Sargasso Sea, mixed-layer TPP averaged 15 ± 1.1 nmol·L^{-1}, with P-lipids contributing 1.3 ± 0.17 nmol·L^{-1}, or 8.4%. Further, C:P was 200 in the Sargasso Sea, with 3.0 μmol·L^{-1} POC, but only 106 in the TWNA, with 14 μmol·L^{-1} POC (Table S1). Without P-sparing strategies, such that Sargasso Sea C:P was also 106, TPP would be 28 nmol·L^{-1}, given 3.0 μmol·L^{-1} POC. Because observed TPP is only 15 nmol·L^{-1}, the latitudinal C:P gradient is responsible for a 13 nmol·L^{-1} reduction in Sargasso Sea TPP. Without lipid substitution, P-lipids contribute 11% of TPP at a C:P of 106 so, without lipid substitution, one might expect a P-lipid concentration in the Sargasso Sea of 11% × 28 = 3.1 nmol·L^{-1}, indicating that lipid substitution spares 1.8 nmol·L^{-1} in the Sargasso, accounting for 14% of the total TPP reduction. This rough estimate of the role of lipids is in keeping with culture experiments showing that lipid substitution can spare phytoplankton 5–40% of cellular P (9).

Estimating the Percentage of TPP and polyP Stocks Exported per Day. Standing stocks of polyP and TPP were calculated by trapezoidal integration between the surface and 150 m at both sites. We used the observed TPP flux in the Sargasso Sea to calculate the polyP flux that would have been observed if the polyP:TPP of exported material was identical to the surface polyP:TPP (2.0 neq·$nmol^{-1}$). We found that polyP flux would have been 11 ± 4 μeq·m^{-2}·d^{-1} in the Sargasso Sea, meaning that, in the absence of preferential polyP recycling, 0.45% ± 0.16% of the 0–150 m polyP standing stock would have been exported per day, which is threefold higher than the actually observed value of 0.14% ± 0.02%. Thus, although it is possible that a greater percentage of the 0–150 m standing stock of TPP and polyP were exported in the Sargasso Sea than in the TWNA, we estimate that the apparent preferential recycling of polyP would have played a significant role in mitigating P loss via sinking particles. However, caution is advised in making quantitative comparisons of this kind between the sediment traps and the surface standing stocks: possible collection biases of this type of sediment trap are unknown, and, because of the high seasonality especially in the TWNA, our samples probably do not represent annual mean conditions.

1. Karl DM, Tien G (1992) MAGIC: A sensitive and precise method for measuring dissolved phosphorus in aquatic environments. *Limnol Oceanogr* 37(1):105–116.
2. Peterson ML, Wakeham SG, Lee C, Askea MA, Miquel JC (2005) Novel techniques for collection of sinking particles in the ocean and determining their settling rates. *Limnol Oceanogr Methods* 3:520–532.
3. Lomas MW, et al. (2013) Two decades and counting: 24-years of sustained open ocean biogeochemical measurements in the Sargasso Sea. *Deep Sea Res Part II Top Stud Oceanogr* 93:16–32.
4. Casey JR, Lomas MW, Mandecki J, Walker DE (2007) *Prochlorococcus* contributes to new production in the Sargasso Sea deep chlorophyll maximum. *Geophys Res Lett* 34:L10604.
5. Casey JR, et al. (2009) Phytoplankton taxon-specific orthophosphate (Pi) and ATP utilization in the western subtropical North Atlantic. *Aquat Microb Ecol* 58:31–44.
6. Martiny AC, et al. (2013) Strong latitudinal patterns in the elemental ratios of marine plankton and organic matter. *Nat Geosci* 6:279–283.
7. Twining BS, Nunez-Milland D, Vogt S, Johnson RS, Sedwick PN (2010) Variations in *Synechococcus* cell quotas of phosphorus, sulfur, manganese, iron, nickel, and zinc within mesoscale eddies in the Sargasso Sea. *Limnol Oceanogr* 55(2):492–506.
8. Popendorf KJ, Fredricks HF, Van Mooy BAS (2013) Molecular ion-independent quantification of polar glycerolipid classes in marine plankton using triple quadrupole MS. *Lipids* 48(2):185–195.
9. Van Mooy BAS, et al. (2009) Phytoplankton in the ocean use non-phosphorus lipids in response to phosphorus scarcity. *Nature* 458(7234):69–72.
10. Suzumura M (2008) Persulfate chemical wet oxidation method for the determination of particulate phosphorus in comparison with a high-temperature dry combustion method. *Limnol Oceanogr Methods* 6:619–629.
11. Dyhrman ST, Ruttenberg KC (2006) Presence and regulation of alkaline phosphatase activity in eukaryotic phytoplankton from the coastal ocean: Implications for dissolved organic phosphorus remineralization. *Limnol Oceanogr* 51(3):1381–1390.
12. Martin P, Van Mooy BAS (2013) Fluorometric quantification of polyphosphate in environmental plankton samples: Extraction protocols, matrix effects, and nucleic acid interference. *Appl Environ Microbiol* 79(1):273–281.
13. Correll DL (1965) Ribonucleic acid-polyphosphate from algae III. Hydrolysis studies. *Plant Cell Physiol* 6:661–669.
14. Diaz JM, Ingall ED (2010) Fluorometric quantification of natural inorganic polyphosphate. *Environ Sci Technol* 44(12):4665–4671.
15. Kulaev IS, Vagabov VM, Kulakovskaya TV (2004) *The Biochemistry of Inorganic Polyphosphates* (Wiley, New York), 2nd Ed, p 277.

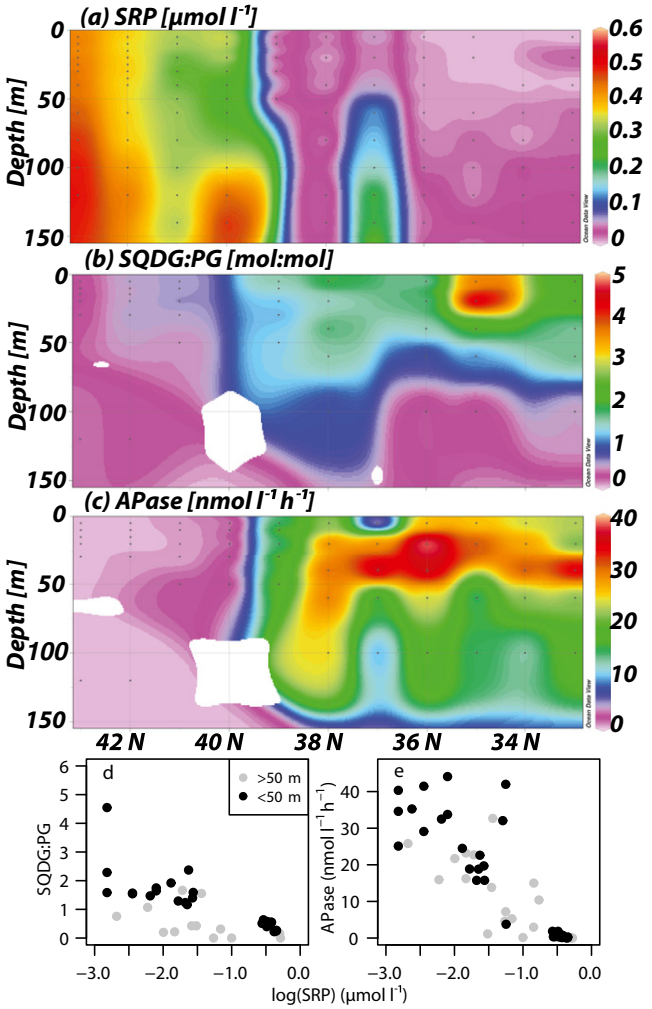

Fig. S1. Sectional data from an April 2008 cruise along 65°W. As on the 2012 cruise, a strong southward decrease in (*A*) SRP, and a concomitant rise in (*B*) SQDG:PG and (*C*) alkaline phosphatase activity were identified. There were significant inverse correlations between both (*D*) SQDG:PG and (*E*) APase against SRP. Because lipid samples were filtered onto 0.2 µm PVDF filters on this cruise, the SQDG:PG ratios were overall lower than in the GF/F-filtered samples collected during April 2012. This difference is most probably because GF/F filters do not quantitatively retain the PG-rich but SQDG-poor heterotrophic bacteria (2).

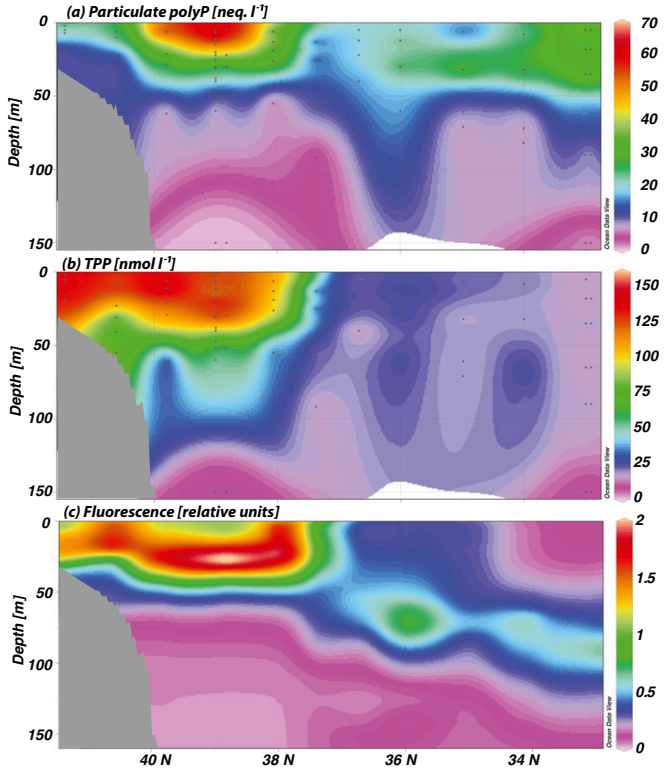

Fig. S2. Sectional data from an April 2012 cruise from Woods Hole to Bermuda, showing the absolute concentrations of (*A*) particulate polyP, (*B*) total particulate phosphorus, and (*C*) relative fluorescence as measured by the fluorometer on the CTD rosette.

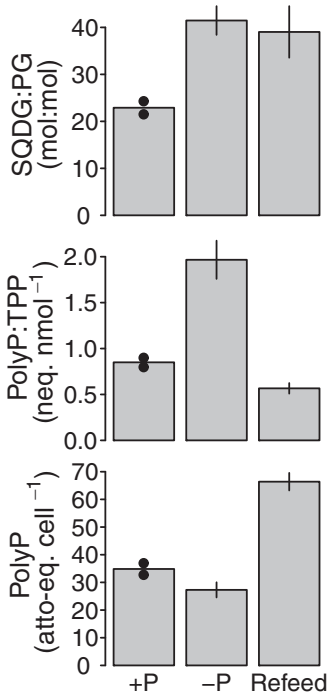

Fig. S3. (*A*) Sulfolipid-to-phospholipid ratio, (*B*) polyphosphate-to-total particulate phosphorus ratio, and (*C*) polyphosphate-per-cell content in batch cultures of the cyanobacterium *Synechococcus* WH8102. *+P*, P-replete cultures; *–P*, P-limited cultures; Refeed, P-limited cultures resupplied with P 24 h before sampling. Bars are means of three (–P and Refeed) or two replicate cultures (+P). For –P and Refeed, error bars indicate one SD; for +P, the data from each replicate are indicated by the points.

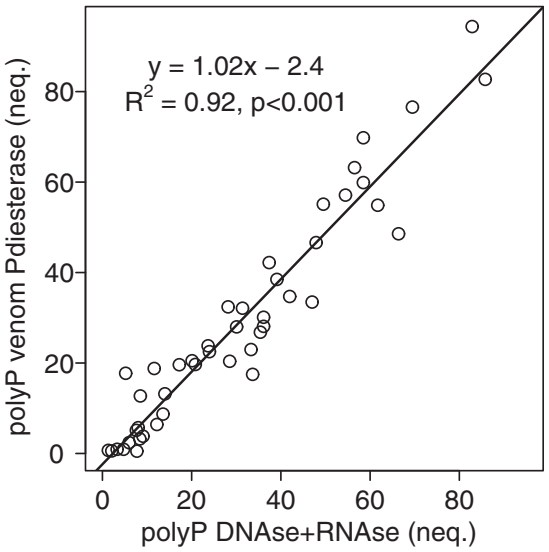

Fig. S4. Using two different enzymatic digestions to determine polyphosphate in the April 2012 cruise samples (venom phosphodiesterase digestion versus DNase+RNase digestion) yielded a relationship indistinguishable from a 1:1 line with only modest scatter.

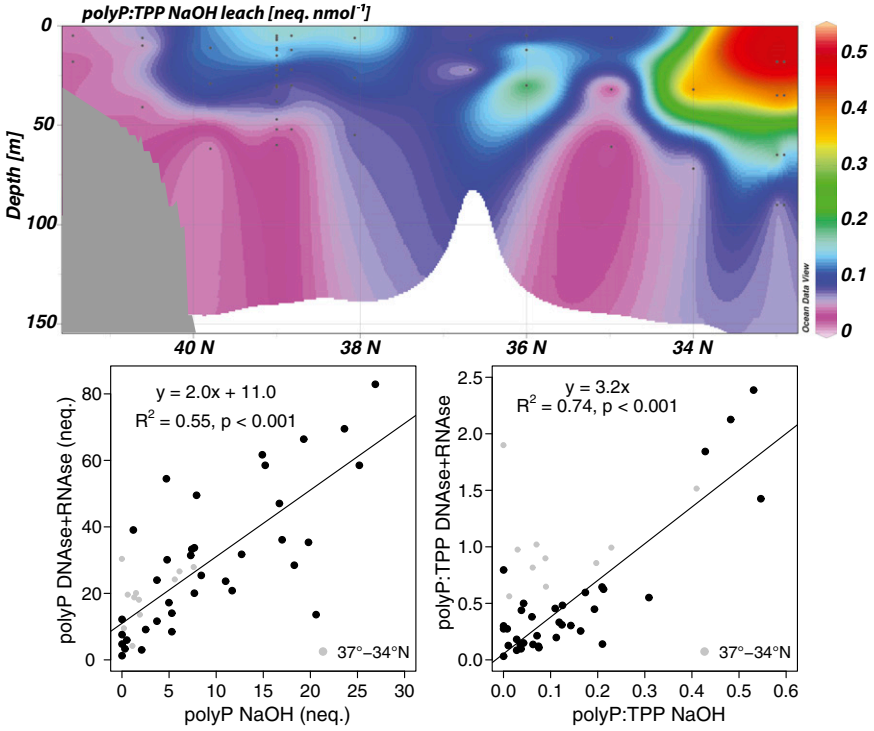

Fig. S5. Using an alternative method to measure polyP based on NaOH extraction yielded lower polyP values, but a latitudinal trend identical to that observed with our enzymatic method. Note that measurements using NaOH between 37°N and 34°N were probably biased low by the very small sample quantities available, which yielded signals very close to blank levels. These data were therefore excluded from the regressions in the two *Lower* panels.

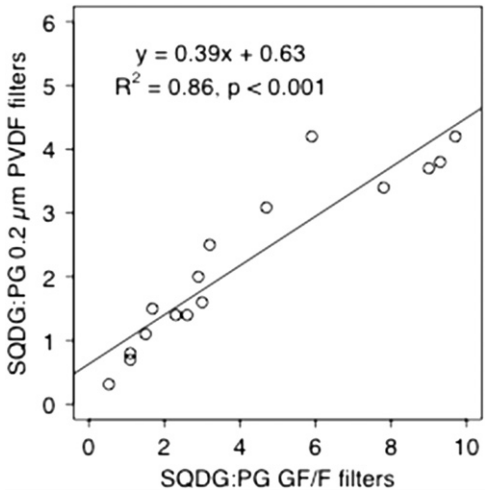

Fig. S6. Relationship between the sulfo-to-phospholipid ratio (SQDG:PG) measured in samples filtered onto 0.2-μm PVDF filters and onto GF/F filters across the April 2012 transect. Data are from temperate and subtropical waters.

Table S1. Surface concentrations of POC, TPP, lipid-P, and polyP in the temperate western North Atlantic (TWNA, 39°N, 0–30 m average) and the Sargasso Sea (33°N, 0–65 m average), integrated water-column inventories of TPP and polyP (0–150 m), and downward fluxes of TPP, polyP, and POC at 150 m

Measured parameter	TWNA, 39°N 69°W			Sargasso Sea, 33°N 66°W		
POC, μmol·L^{-1}	14 ± 1.4			3.0 ± 0.46		
TPP, nmol·L^{-1}	130 ± 17			15 ± 1.1		
POC:TPP, mol·mol^{-1}	106 ± 11			200 ± 33		
Lipid-P, nmol·L^{-1}	15 ± 1.1			1.3 ± 0.17		
PolyP, neq·L^{-1}	49 ± 18			30 ± 9.4		
Lipid-P, percent of TPP	11 ± 1.4			8.4 ± 1.0		
PolyP:TPP, neq·nmol^{-1}	0.39 ± 0.17			2.0 ± 0.68		
TPP integrated stock, μmol·m^{-2}	8,690 ± 1,540			2,230 ± 330		
PolyP integrated stock, μeq·m^{-2}	2,170 ± 490			2,490 ± 410		
	Trap 1	Trap 2	Trap 3	Trap 1	Trap 2	Trap 3
Trap TPP flux, μmol·m^{-2}·d^{-1}	6.2	7.2	4.1	4.8	7.8	4.0
Trap polyP flux, μeq·m^{-2}·d^{-1}	2.1	2.1	1.6	4.2	3.6	3.0
Trap polyP:TPP, neq·nmol^{-1}	0.34	0.29	0.39	0.88	0.46	0.75
% of TPP stock exported d^{-1}	0.07	0.08	0.05	0.22	0.35	0.18
% of polyP stock exported d^{-1}	0.10	0.10	0.07	0.17	0.14	0.12
Trap POC flux, mmol C·m^{-2}·d^{-1}	1.43 ± 0.69			0.86 ± 0.20		

Concentrations and water-column inventories (mean ± SD) were calculated from two to three replicate profiles taken at the same station as the trap deployments. The absolute values of fluxes should be interpreted with caution because collection biases of the surface-tethered, wide-aperture net traps used in this study are unknown. Moreover, the fluxes do not represent the full range of seasonal variability, especially not in the TWNA. Note that POC fluxes were measured on additional deployments of identical traps at each site so only average POC fluxes are reported. μeq, microequivalents; neq, nanoequivalents; POC, particulate organic carbon; polyP, polyphosphate; TPP, total particulate P.